CHEMICAL ENGINEERING TRANSACTIONS
VOL. 88, 2021
A publication of AIDIC
The Italian Association of Chemical Engineering
Online at www.cetjournal.it
Guest Editors: Petar S. Varbanov, Yee Van Fan, Jiří J. Klemeš

ISBN 978-88-95608-86-0; **ISSN** 2283-9216
DOI: 10.3303/CET2188072

Performance Assessment of Solid Oxide Electrolysis Cells Based on Different Electrolytes for Syngas Production

Dang Saebea[a], Amornchai Arpornwichanop[b], Yaneeporn Patcharavorachot[c,*]

[a] Reasearch Unit of Developing technology and Innovation of Alternative Energy for Industries, Department of Chemical Engineering, Faculty of Engineering, Burapha University, Chonburi, 20131, Thailand
[b] Center of Excellence in Process and Energy Systems Engineering, Department of Chemical Engineering, Faculty of Engineering, Chulalongkorn University, Bangkok 10330, Thailand
[c] Department of Chemical Engineering, Faculty of Engineering, King Mongkut's Institute of Technology Ladkrabang, Bangkok 10520, Thailand
yaneepon.p@hotmail.com

The development of solid oxide electrolysis cell (SOEC) for syngas production has achieved considerable attention because SOEC can directly convert carbon dioxide (CO_2) to carbon monoxide (CO). The material of electrolyte for SOEC has a significant effect on the cell performance. Y_2O_3-stabilized ZrO_2 (YSZ) and Sr- and Mg-doped $LaGaO_3$ (LSGM) are interesting electrolytes for SOEC due to their high oxide ion conductivity. Therefore, this work aims to simulate and study the SOECs with YSZ-based and LSGM-based electrolytes by H_2O/CO_2 co-electrolysis for syngas production. The predicted results of both SOEC models were in good agreement with experiment data. The validated models of both SOECs were used to analyze the effect of temperature. The increase of operating temperature can reduce the cell voltage and power consumption of both SOECs. When comparing both SOECs, the cell voltage of YSZ-SOEC is lower than that of LSGM-SOEC in the range of 800-1,000 °C. On the other hand, the performance of LSGM-SOEC is superior to that of YSZ-SOEC at an operating temperature below 800 °C.

1. Introduction

Nowadays global energy consumption is increasing rapidly while fossil energy sources are decreasing. Moreover, the use of fossil fuel is the main cause of the CO_2 and greenhouse gas emissions in the atmosphere which are the major environmental problems. Renewable energies, i.e., solar, wind, and nuclear that are sustainable and environment-friendly resources have attracted much attention. However, these renewable sources result in unstable capacity of electricity production because they depend on the weather condition and other uncontrollable factors. Therefore, they require the use of an on-site energy storage system. Electrolyzer is an attractive energy storage device for the conversion of power to fuel. The electrolyzer can produce hydrogen from splitting water with electricity.

Solid oxide electrolysis cell (SOEC) is regarded as a promising technology for fuel production owing to its high efficiency and durability. Grigoriev et al. (2020) reported that theoretical efficiency of SOEC is above 80%. SOEC is higher than the efficiency of alkaline electrolysis cell (AEC) and proton exchange membrane electrolysis cell (PEMEC). Moreover, SOEC not only produces hydrogen via steam electrolysis, but it can also convert CO_2 to CO. Currently, the utilization of CO_2 has been proposed to reduce CO_2 emissions (Zhang et., 2017). Thus, SOEC is an interesting alternative because it can produce fuel and reduce CO_2 emissions.

Although CO_2 can be converted to CO in SOEC, the carbon deposition on cathode side suffers from CO_2 electrolysis of SOEC (Saebea et al., 2017). The co-electrolysis of H_2O and CO_2 alleviates the problem of carbon formation. Furthermore, the H_2O and CO_2 co-electrolysis has faster reaction rate, lower cell resistance, and lower power consumption than CO_2 electrolysis (Menon et al., 2015). The syngas is produced from SOEC in H_2O and CO_2 co-electrolysis mode. H_2 and CO in syngas are important feedstocks for the production of various chemicals and fuels such as synthetic diesel via Fischer-Tropsch synthesis, or methane, methanol, and dimethyl ether via catalytic reactions (Rivera-Tinoco et al., 2016).

Paper Received: 8 June 2021; Revised: 20 September 2021; Accepted: 6 October 2021
Please cite this article as: Saebea D., Arpornwichanop A., Patcharavorachot Y., 2021, Performance Assessment of Solid Oxide Electrolysis Cells Based on Different Electrolytes for Syngas Production, Chemical Engineering Transactions, 88, 433-438 DOI:10.3303/CET2188072

In general, yttria-stabilized zirconia (YSZ) is applied as electrolyte of SOEC due to its high ion conductivity, stability on reactions of oxidation and reduction, and mechanical strength. The SOEC with YSZ-based electrolyte needs to operate at high temperature in range of 800-1000 °C. The cell operation under high temperature causes thermal gradient and thermal shock resistance, resulting in the short lifetime (Petipas et al., 2017). A candidate for SOEC electrolyte is a strontium and magnesium doped lanthanum gallate ($La_{0.9}Sr_{0.1}Ga_{0.8}Mg_{0.2}O_3$, LSGM) which has high oxide ion conductivity and ionic transport number (Ishihara et al., 2017). The SOECs with YSZ-based and LSGM-based electrolytes have different advantages and disadvantages. In syngas production, the SOECs by H_2O and CO_2 co-electrolysis mode is rather complex. The suitable operation of SOECs with YSZ-based and LSGM-based electrolytes for H_2O and CO_2 co-electrolysis should be investigated. To compare their behavior and performance in all aspects, the mathematical model can help to study the internal working of cell and predict the appropriate operating condition.Thus, the mathematical models of YSZ-SOEC and LSGM-SOEC for H_2O/CO_2 co-electrolysis that combine electro-chemistry, porous media transport, and mass transport are studied this work. Moreover, the performance of SOECs with YSZ-based and LSGM-based electrolytes is studied and compared.

2. SOEC Model

The SOEC consists of three main components, i.e., cathode, electrolyte, and anode. The SOECs with YSZ-based and LSGM-based electrolytes are studied in this work. In the structure of SOEC with YSZ-based electrolyte, nickel–yttria stabilized zirconia (Ni-YSZ) and Sr-doped $LaMnO_3$ (LSM) are considered as cathode and anode, respectively. For SOEC with LSGM-based electrolyte, materials of cathode and anode are nickel-$La_{0.9}Sr_{0.1}Ga_{0.8}Mg_{0.8}O_{3-\delta}$ (Ni-LSGM) and $La_{0.6}Sr_{0.4}Co_{0.2}Fe_{0.8}O_3$-$Ce_{0.9}Gd_{0.1}O_{1.95}$ (LSCF-GDC), respectively.

2.1 SOEC operation

Steam and carbon dioxide are fed to cathode side. H_2O electrolysis, CO_2 electrolysis, and reverse water gas-shift reactions in Eqs(1)-(3) occur at the triple-phase boundary between cathode and electrolyte. The oxygen ions diffuse through electrolyte from the cathode-electrolyte interface to the anode-electrolyte interface. The oxygen ions form to oxygen molecules at the anode side, as shown in Eq(4). Air is introduced to the anode side and sweeps the oxygen molecule.

$$H_2O + 2e^- \leftrightarrow H_2 + O^{2-} \tag{1}$$

$$CO_2 + 2e^- \leftrightarrow CO + O^{2-} \tag{2}$$

$$CO_2 + H_2 \leftrightarrow CO + H_2O \tag{3}$$

$$O^{2-} \rightarrow \frac{1}{2}O_2 + 2e^- \tag{4}$$

To simulate SOEC behaviour, the assumptions used for the model of SOEC by H_2O and CO_2 co-electrolysis are the following:
(1) All gases are ideal.
(2) SOEC is operated at steady-state and isothermal conditions.
(3) Pressure drop and temperature gradient in the SOEC are negligible.
(4) The reaction sites at electrode/electrolyte interface are uniformly distributed.

2.2 Electrochemical model

Power input is required for the co-electrolysis of H_2O and CO_2. The power consumption of SOEC relates to current density and operating cell voltage. The total current density is the sum of charge transfers for H_2O electrolysis and CO_2 electrolysis as shown in Eq(5).

$$j = j_{H_2} + j_{CO} = \varepsilon j + (1-\varepsilon) j \tag{5}$$

where ε is the normalization factor which is the ratio of H_2 electrochemical current density at the cathode-electrolyte interface to total current density. For the operation of SOEC, the operating cell voltage is the sum of reversible and irreversible potentials as follows:

$$V_{cell} = E + \eta_{act,ca} + \eta_{act,an} + \eta_{ohm} \tag{6}$$

where $\eta_{act,ca}$ and $\eta_{act,an}$ are the activation polarizations of cathode and anode (V), respectively, η_{ohm} is the ohmic polarization (V), and E is the reversible cell voltage (V) which is a minimum potential at open-circuit condition expressed by the Nernst equation in Eq(7) and Eq(8).

$$E_{2} = E^{0}_{H_2} + \frac{RT}{2F}\ln\left(\frac{p_{2}(p_{O_2})^{\frac{1}{2}}}{H_2O}\right) \tag{7}$$

$$E_{CO} = E^{0}_{CO} + \frac{RT}{2}\ln\left(\frac{p_{CO}(p_{O_2})^{\frac{1}{2}}}{p_{CO_2}}\right) \tag{8}$$

where E^{0}_{i} is the reversible cell voltage at standard pressure (V), p_i is the partial pressure of species i at electrode-electrolyte interface (bar), *F* is the Faraday constant (C.mol^{-1}), and *R* is the gas constant (J.mol^{-1}.K^{-1}). Activation polarizations which are related to the sluggishness of the electrolysis reaction at the electrode/electrolyte interfaces can be described by Butler–Volmer equation. Activation overpotentials occurring from H_2O electrolysis at anode and cathode are shown in Eq(9) and Eq(10), respectively. Eq(11) and Eq(12) show the activation overpotentials for CO_2 electrolysis at anode and cathode, respectively.

$$j_{H_2} = j^{0}_{H_2}\left|\exp\left(\frac{(1+\beta_{an})F\eta_{act,ca}}{RT}\right) - \exp\left(-\frac{\beta_{ca}F\eta_{act,ca}}{RT}\right)\right| \tag{9}$$

$$H_2 = j^{0}_{O_2}\ \exp\left(\frac{\beta_{an}F\eta_{act,ca}}{RT}\right) - \exp\left(-\frac{\beta_{ca}F\eta_{act,an}}{RT}\right)\Bigg| \tag{10}$$

$$j_{CO} = j^{0}_{CO}\,|\exp\left(\frac{\beta_{an}\ \eta_{act,ca}}{RT}\right) - \exp\left(-\frac{(1+\beta_{ca})F\eta_{act,ca}}{RT}\right)\Bigg| \tag{11}$$

$$j_{CO} = j^{0}_{O_2}\ \exp\left(\frac{\beta_{an}F\eta_{act,ca}}{RT}\right) - \exp\left(-\frac{\beta_{ca}F\eta_{act,an}}{RT}\right)\Bigg| \tag{12}$$

where β_{an} and β_{ca} are the asymmetric charge transfer coefficients at anode and cathode, respectively, and $j^{0}_{H_2}$, j^{0}_{CO}, and $j^{0}_{O_2}$ are the exchange current densities of H_2, CO, and O_2 (A.m^{-2}), respectively, which are related to open surface coverage and surface coverage of electrochemically active species, as shown in Eqs(13)-(15).

$$j_{H_2} = j^{*}_{H_2O}\frac{\left(\frac{p_{H_2}}{p^{*}_{H_2}}\right)^{\frac{1}{4}}\left(p_{H_2O}\right)^{\frac{3}{4}}}{1+\left|\frac{p_{H_2}}{p^{*}_{H_2}}\right)^{\frac{1}{2}}} \tag{13}$$

$$j^{0}_{CO} = j^{*}_{CO_2}\frac{\left(\frac{p_{CO_2}}{p^{*}_{CO}}\right)^{\frac{1}{4}}}{1\ \left(\frac{p_{CO}}{p^{*}_{CO}}\right)+\left(\frac{p_{CO}}{p^{*}_{CO_2}}\right)} \tag{14}$$

$$j_{O_2} = j^{*}_{H_2O}\frac{\left(\frac{p_{O_2}}{p^{*}_{O_2}}\right)^{\frac{1}{4}}}{1+\left|\frac{p_{O_2}}{p^{*}_{O_2}}\right)^{\frac{1}{2}}} \tag{15}$$

where p_i^* is partial pressure of species i at equilibrium condition (bar), j_i^0 is the exchange current density of species i (A.m^{-2}) which can be expressed by the Arrhenius law, and j_i^* is the current density of species i at equilibrium condition (A.m^{-2}).

Ohmic polarization occurs from resistance along the ionic flow in the electrolyte and the electron flow though the anode and cathode. The ohmic polarization is expressed by Ohm's law as follows:

$$\eta_{ohm} = R_t j \tag{16}$$

where R_i is the electronic and ionic resistances (Ω) which are function of conductivity and thickness of the individual layers.

2.3 Mass balance for porous transport

The concentration of gas in the porous electrode is considered from mass balance equation in Eq(17). Dusty-gas model is used for the reactive transport of multi-component gas, as expressed by Eq(18).

$$\frac{\varepsilon}{RT}\frac{\partial(y_i P)}{\partial t} = -\nabla N_i + R_i \tag{17}$$

$$\frac{N_i}{D_{i,k}^{eff}} + \sum_{j=1, j\neq 1}^{n} \frac{y_j N_i - y_i N_j}{D_{ij}^{eff}} = -\frac{P}{RT}\frac{dy_i}{dx} \tag{18}$$

where ε is the electrode porosity, y_i is the mole fraction of species i, N_i is the molar flux of species i, R_i is the reaction rate of species i, $D_{i,k}^{eff}$ is the effective Knudsen diffusion coefficient, and D_{ij}^{eff} is the effective binary diffusion coefficient.

3. Results and discussion

3.1 Validation of model

Eqs(5)-(18) from the previous section were used for simulating the performances of YSZ-SOEC and LSGM-SOEC. The nonlinear algebraic equations of SOEC model were solved by using MATLAB. Due to different anode, cathode, and electrolyte materials of both SOECs, the material property values of both SOECs such as porosity, tortuosity factor, conductivities, and pre-exponent factors, are dissimilar. The material property parameters of both SOECs are included in Table 1.

Table 1: *Values of the material property parameters for the SOEC.*

Parameters	YSZ-SOEC	LSGM-SOEC
Cathode porosity	0.5	0.26
Anode porosity	0.5	0.3
Tortuosity factor	5	3
Cathode conductivity (S.m^{-1})	$3.27\times10^6 - 1065.3T$	1×10^3
Anode conductivity (S.m^{-1})	$\frac{4.2\times10^7}{T}\exp\left(-\frac{1150}{T}\right)$	3×10^4
Electrolyte conductivity (S m^{-1})	$3.27\times10^6 - 1065T$	$\frac{5.17\times10^8}{T}\exp\left(-\frac{93800}{RT}\right)$
Pre-exponent factor of H_2 (k)	6.0 x 10^{10}	6.0 x 10^{10}
Pre-exponent factor of CO (k)	1.2 x 10^{10}	1.2 x 10^{10}
Pre-exponent factor of O_2 (k)	4.0 x 10^{12}	5.0 x 10^{12}

To ensure the reliability of the simulated model of both SOECs, the voltage as a function of current density from the model of SOEC with YSZ-based electrolyte was verified with experimental data of Ni (2012). For the LSGM-SOEC model, the results from model prediction were compared with the experimental data reported by Wendel et al. (2015). The operating and configuration parameters for the model validation of both SOECs are included in Table 2. The operating temperature of YSZ-SOEC is 800 °C while the LSGM-SOEC is operated at 650 °C. Figures 1a and 1b show the comparison of cell voltage at various current densities in the range of 0-10,000 A.m^{-2} between predictions and experimental results of YSZ-SOEC and LSGM-SOEC, respectively. From Figure 1,

the cell voltage is enhanced with increasing the current density. The current-voltage characteristics of YSZ-SOEC and LSGM-SOEC are the same tendency. Figures 1a and 1b can show that the simulated results from both models fit well with the experimental data**.** Root mean square errors (R^2) are 0.992 for YSZ-SOEC and 0.997 for LSGM-SOEC. The R^2 values of both SOEC models are close to 1. This indicates that the results from predictions of both models are reliable.

Table 2: Operating and configuration parameters for the model validation.

Parameters	YSZ-SOEC	LSGM-SOEC
Operating temperature (°C)	800	650
Pressure (bar)	1	1
Inlet gas composition at anode channel	49.7% H_2O, 25% CO_2, 25% H_2, and 3% CO	50% H_2O, 0% CO_2, 50% H_2, and 0% CO
Inlet gas compositions at cathode channel	21% O_2, 79% N_2	21% O_2, 79% N_2
Cathode thickness (μm)	500	600
Anode thickness (μm)	50	20
Electrolyte thickness (μm)	50	16

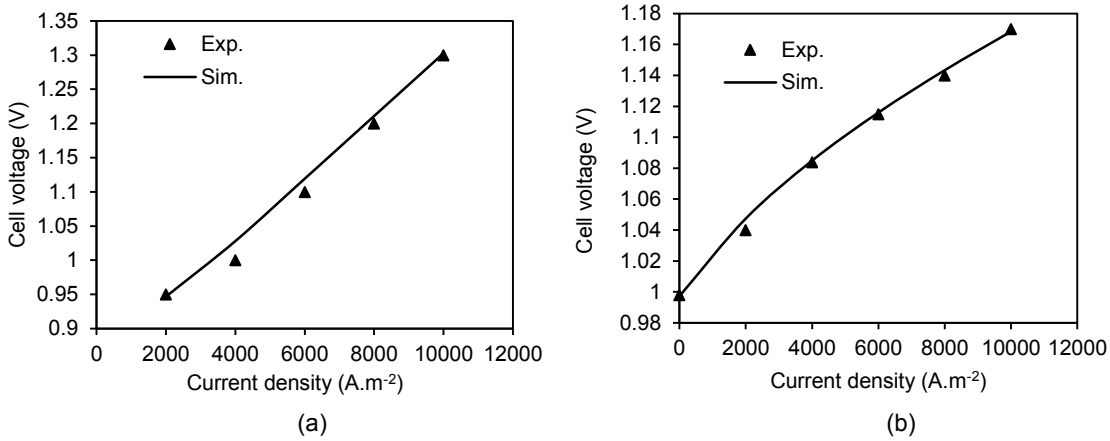

Figure 1: *Comparison between the predicted results from SOEC model and the experimental results* (*a) YSZ-SOEC and* (*b) LSGM-SOEC*.

3.2 Comparison of YSZ-SOEC and LSGM-SOEC

The validated models of YSZ-SOEC and LSGM-SOEC were used for studying their performance. In the investigation of their performance, the YSZ-SOEC and LSGM-SOEC are based on the cathode-supported structure. The components of inlet cathode gas are 45% for H_2O, 45% for CO_2, and 10% for H_2. In the anode side, air is fed.

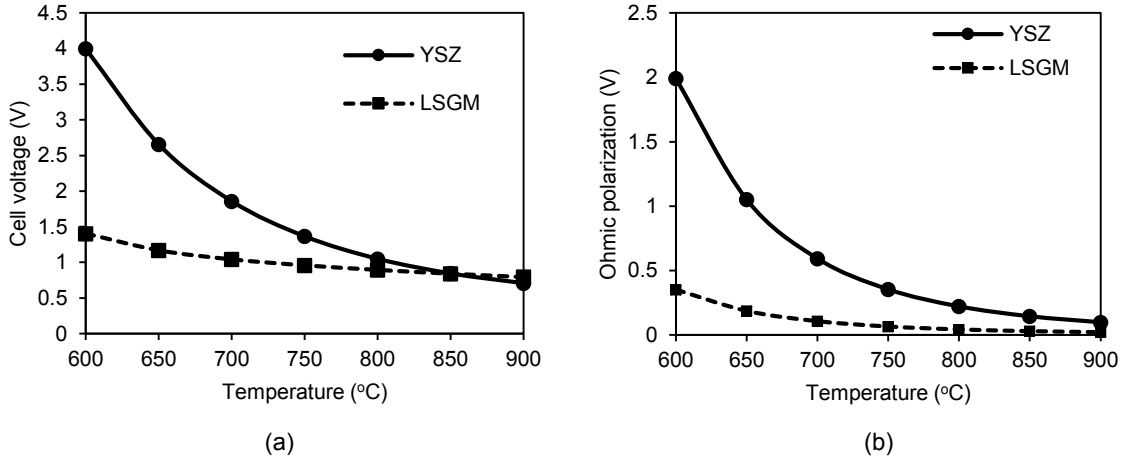

Figure 2: *Effect of operating temperature on* (*a*) *cell voltage and* (*b*) *Ohmic polarization.*

The influence of operating temperature in the range of 600-900 ºC on the cell voltage of YSZ-SOEC and LSGM-SOEC at the current density of 10,000 $A.m^{-2}$ is shown in Figure 2a. From Figure 2a, the cell voltage of both SOECs decreases with increasing of operating temperature. The power density directly relates to the cell voltage. This indicates that the power consumption of SOECs for H_2O/CO_2 co-electrolysis reduces at higher operating temperatures. It can be explained that the increase of operating temperature results in the reduction of reversible voltage and ohmic polarization as shown in Figure 2b. Consequently, this leads to the decrease in the cell voltage. In the range of 600-800 ºC, the cell voltage of YSZ-SOEC vastly reduces. For the LSGM-SOEC, the increase of operating temperature has an insignificant effect on the cell voltage. When comparing the two types of SOECs, the cell voltage of LSGM-SOEC is lower than that of YSZ-SOEC at a low temperature of 600-850 ºC**.** At the operating temperature above 850 ºC, the cell voltage of LSGM-SOEC is slightly higher than that of YSZ-SOEC. This indicates that the conductivity of LSGM electrolyte at low temperature is substantially higher than that of YSZ electrolyte**.** Thus, the ohmic polarization of LSGM-SOEC is obviously lower than that of YSZ-SOEC at low temperatures**.** Figure 2a indicates that the cell voltage of LSGM-SOEC at 700 ºC is close to that of YSZ-SOEC at 800 ºC. The power densities of LSGM-SOEC at 700 ºC and YSZ-SOEC at 800 ºC are 10.41 and 10.48 $kW.m^{-2}$, respectively**.**

4. Conclusions

The performances of SOECs with YSZ-based electrolyte and LSGM-based electrolyte for H_2O and CO_2 co-electrolysis have been presented. The models of YSZ-SOEC and LSGM-SOEC were verified with the experimental data in order to ensure the accuracy of the results. The results from the simulation of both SOEC models showed good agreement with experimental data. The verified models were used for studying the effect of operating temperature on the cell performance of both SOECs. The cell voltage of SOECs can reduce with increase in the operating temperature. When comparing YSZ-SOEC and LSGM-SOEC, the increase of operating temperature on the performance of YSZ-SOEC has more effect than that of LSGM-SOEC. In the range of 600 to 850 ºC, the power consumption of LSGM-SOEC for H_2O and CO_2 co-electrolysis is lower than that of YSZ-SOEC. However, the increase of temperature above 850 ºC considerably affects on the reduction of ohmic potential in the YSZ-SOEC. Thus, YSZ-SOEC consumes less power than LSGM-SOEC at high temperatures.

Acknowledgements

The authors gratefully acknowledge the Research and Innovation Administration Division and Faculty of Engineering, Burapha University.

References

Grigoriev S.A., Fateev V.N., Bessarabov D.G., Millet P., 2020, Current status, research trends, and challenges in water electrolysis science and technology, International Journal of Hydrogen Energy, 45, 26036-26058.

Ishihara T., Wang S., Wu K.T., 2017, Highly active oxide cathode of $La(Sr)Fe(Mn)O_3$ for intermediate temperature CO_2 and CO_2-H_2O co-electrolysis using LSGM electrolyte, Solid State Ionics, 299, 60-63.

Menon V., Fu Q., Janardhanan V.M., Deutschmann Q., 2015, A model-based understanding of solid-oxide electrolysis cells (SOECs) for syngas production by H_2O/CO_2 co-electrolysis, Journal Power Sources, 274, 768-781.

Ni M., 2012, An electrochemical model for syngas production by co-electrolysis of H_2O and CO_2, Journal Power Sources, 202, 209– 216.

Petipas F., Brisse A., Bouallou C., 2017, Thermal Management of Solid Oxide Electrolysis Cell Systems Through Air Flow Regulation, Chemical Engineering Transactions, 61, 1069-1074.

Rivera-Tinoco R., Farran M., Bouallou C., Auprêtre F., Valentin S., Millet P., Ngameni J.R., 2016, Investigation of power-to-methanol processes coupling electrolytic hydrogen production and catalytic CO_2 reduction, International Journal of Hydrogen Energy, 41, 4546-4559.

Saebea D., Authayanun S., Patcharavorachot Y., Soisuwan S., Assabumrungrat S., Arpornwichanop A., 2017, Performance Analysis of Solid-Oxide Electrolysis Cells for Syngas Production by H_2O/CO_2 Co-Electrolysis, Chemical Engineering Transactions, 57, 1627-1632.

Wendel C.H., Gao Z., Scott A.B., Robert J.B., 2015, Modelling and experimental performance of an intermediate temperature reversible solid oxide cell for high-efficiency, distributed-scale electrical energy storage, Journal Power Sources, 283, 329-342.

Zhang X., Song Y., Wang G., Bao X., 2017, Co-electrolysis of CO_2 and H_2O in high-temperature solid oxide electrolysis cells: Recent advance in cathodes, Energy Chemistry, 26, 839-853.